# The first observation of $Na_2TiS_2$ related structure in a two-dimensional anionic manganese trimesate intercalated by cationic imidazole

Partha Mahata and Srinivasan Natarajan*

## ELECTRONIC SUPPLEMENTARY INFORMATION

* Corresponding Authors, E-mail: snatarajan@sscu.iisc.ernet.in

**Table S1**: Crystal data and structure refinement parameters for [HImd][Mn(BTC)($H_2O$)]

| | |
|---|---|
| Empirical formula | [HImd][Mn(BTC)($H_2O$)] |
| Formula weight | 349.16 |
| Crystal system | Monoclinic |
| Space group | $P2_1/c$ (no.14) |
| a (Å) | 6.491(2) |
| b (Å) | 9.599(3) |
| c (Å) | 19.397(6) |
| α (deg) | 90.0 |
| β (deg) | 96.001(5) |
| γ (deg) | 90.0 |
| Volume ($Å^3$) | 1202.0(7) |
| Z | 4 |
| T (K) | 293(2) |
| $\rho_{calc}$ ($g\ cm^{-3}$) | 1.929 |
| μ ($mm^{-1}$) | 1.142 |
| θ range (deg) | 2.11 to 28.04 |
| λ (Mo Kα) (Å) | 0.71073 |
| R indices [I>2σ(I)] | $R_1 = 0.0274$, $wR_2 = 0.0745$ |
| R indices (all data) | $R_1 = 0.0302$, $wR_2 = 0.0763$ |

$R_1 = \Sigma\ ||F_0|-|F_c|| / \Sigma\ |F_0|$; $wR_2 = \{\Sigma[w(F_0^2 - F_c^2)^2] / \Sigma[w(F_0^2)^2]\}^{1/2}$. $w = 1/[\sigma^2(F_0)^2 + (aP)^2 + bP]$, $P = [max.(F_0^2,0) + 2(F_c)^2]/3$, where a = 0.0448 and b = 0.4110.

**Table S2**: Selected bond distances (Å) observed in [HImd][Mn(BTC)($H_2O$)]

| Bond | Amplitude | Bond | Amplitude |
|---|---|---|---|
| Mn(1)-O(1)#1 | 2.0941(13) | Mn(1)-O(4) | 2.2419(14) |
| Mn(1)-O(2)#2 | 2.1457(11) | Mn(1)-O(5)#3 | 2.2490(13) |
| Mn(1)-O(3) | 2.1720(13) | Mn(1)-O(6) | 2.4868(13) |

Symmetry transformations used to generate equivalent atoms:
#1 -x,y-1/2,-z+1/2
#2 x,-y+1/2,z-1/2
#3 -x,y+1/2,-z+1/2

**Table S3**. Selected bond angles observed in [HImd][Mn(BTC)($H_2O$)]

| Angle | Amplitude | Angle | Amplitude |
|---|---|---|---|
| O(1)#1-Mn(1)-O(2)#2 | 123.44(5) | O(2)#2-Mn(1)-O(3) | 144.93(4) |
| O(1)#1-Mn(1)-O(3) | 91.48(5) | O(1)#1-Mn(1)-O(4) | 92.43(6) |
| O(2)#2-Mn(1)-O(4) | 86.88(5) | O(3)-Mn(1)-O(4) | 88.59(5) |
| O(1)#1-Mn(1)-O(5)#3 | 86.04(5) | O(2)#2-Mn(1)-O(5)#3 | 87.48(4) |
| O(3)-Mn(1)-O(5)#3 | 99.21(4) | O(4)-Mn(1)-O(5)#3 | 172.08(4) |
| O(1)#1-Mn(1)-O(6) | 145.38(4) | O(2)#2-Mn(1)-O(6) | 90.40(4) |
| O(3)-Mn(1)-O(6) | 55.70(5) | O(4)-Mn(1)-O(6) | 96.94(5) |
| O(5)#3-Mn(1)-O(6) | 88.66(4) | | |

Symmetry transformations used to generate equivalent atoms:
#1 -x,y-1/2,-z+1/2
#2 x,-y+1/2,z-1/2
#3 -x,y+1/2,-z+1/2

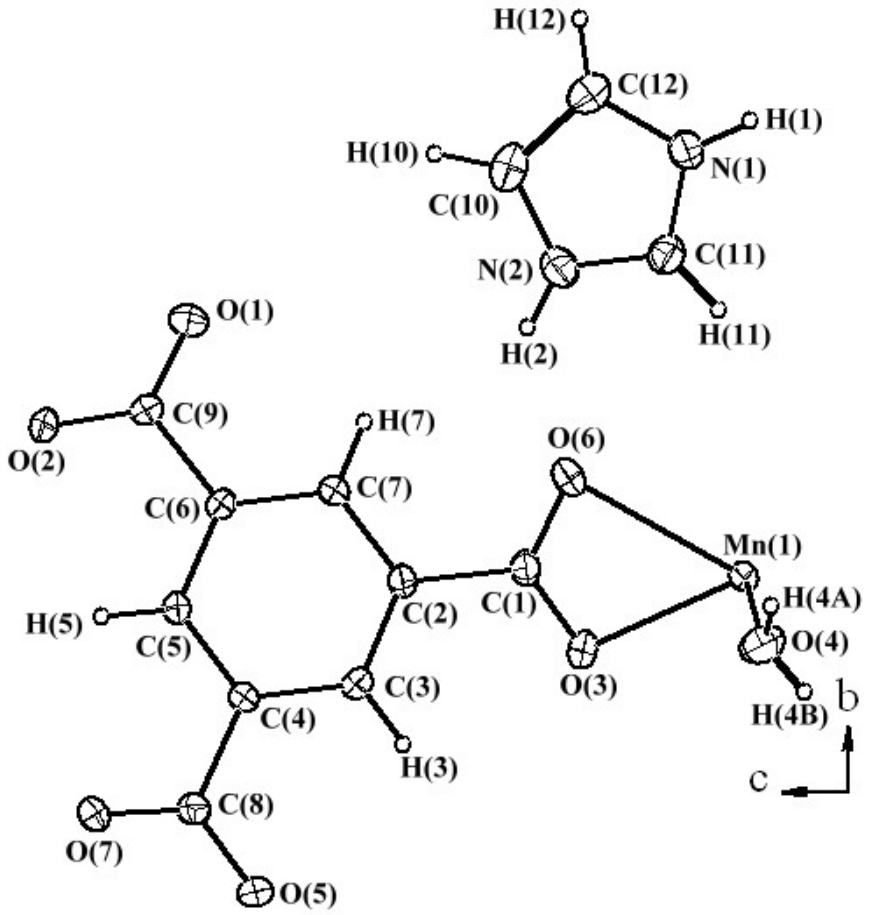


Fig. S1: The asymmetric unit of **I**. Thermal ellipsoids are given at 50% of the probability.

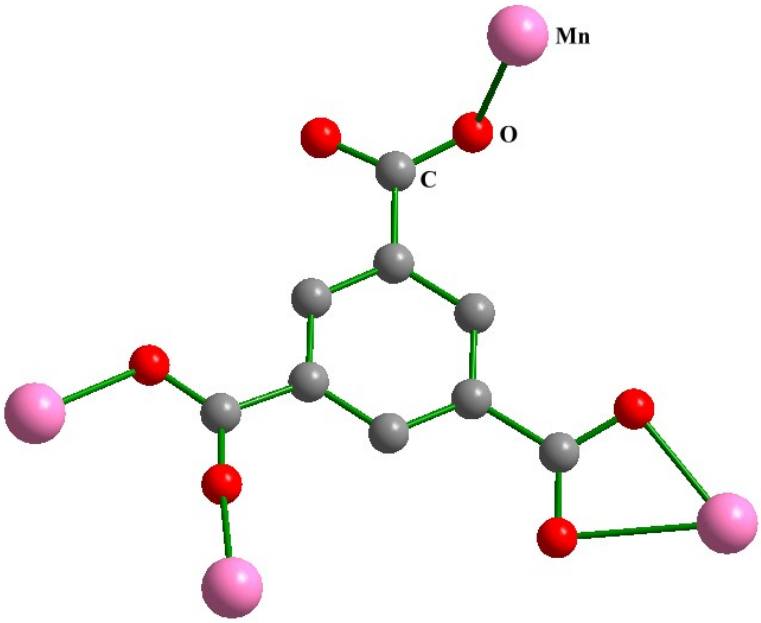


Fig. S2: Figure shows the connectivity of the trimesate anion with $Mn^{+2}$ ions in **I**.

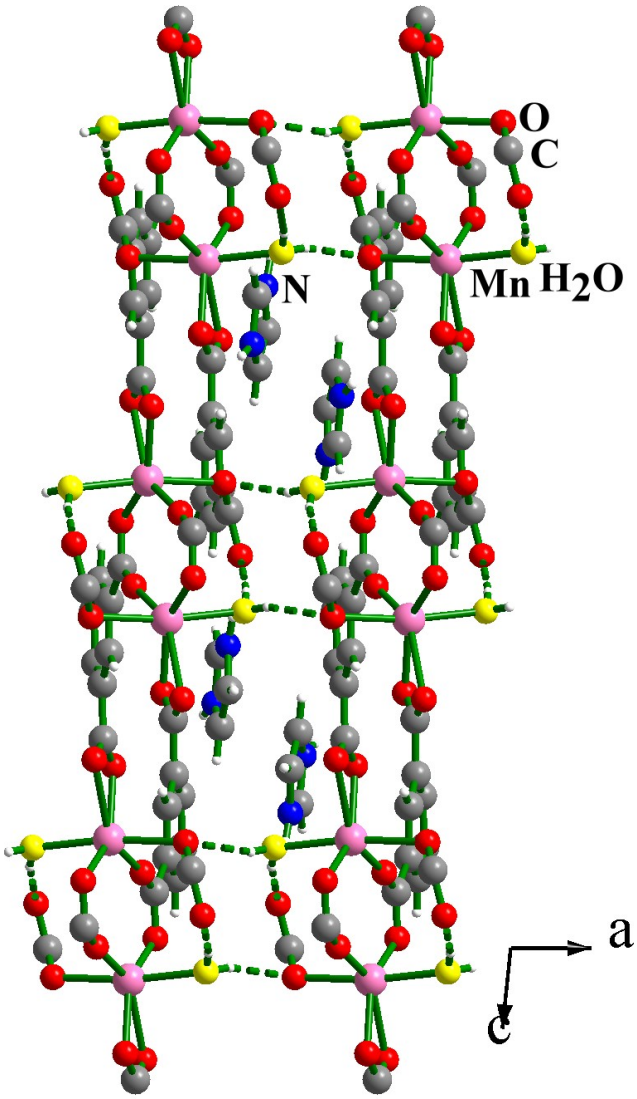


Fig. S3: Figure shows the structure of two layers with inter-layer protonated imidazole molecules and the hydrogen bond interaction between coordinated water molecules and oxygen atom of the carboxylate groups.

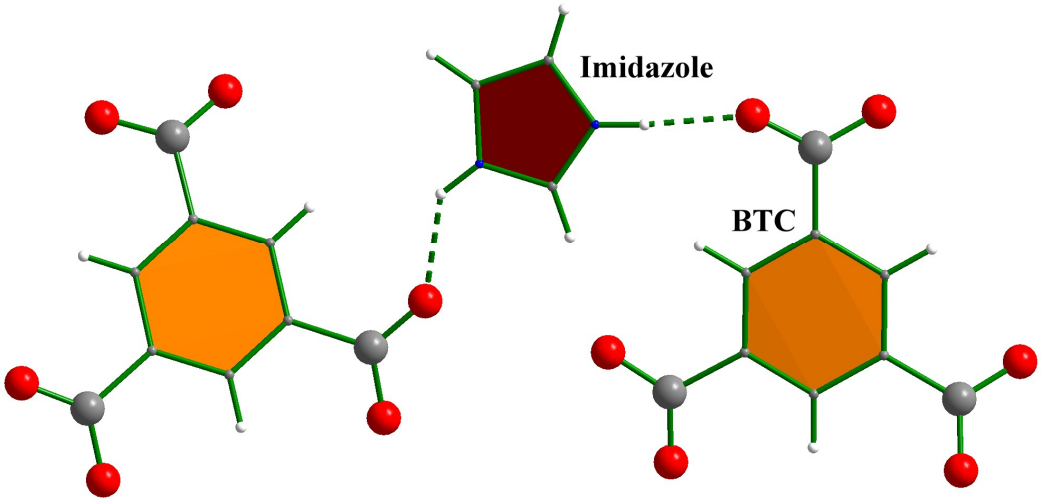


Fig. S4: Figure shows the hydrogen bond interactions between the protonated imidazole molecules and the carboxylate oxygens of the layer.

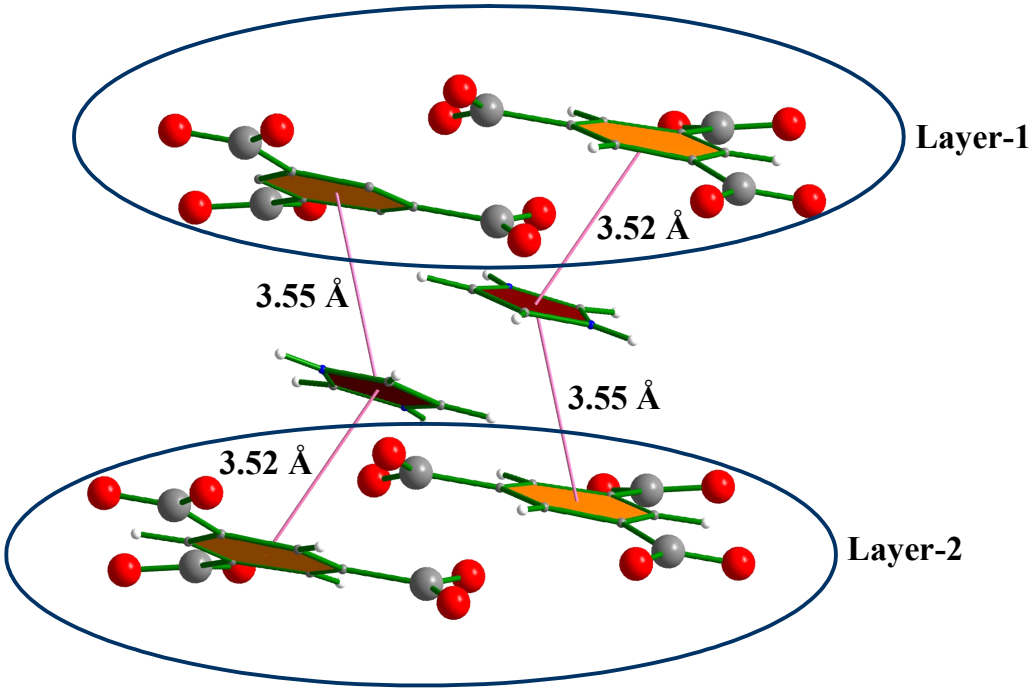


Fig. S5: Figure shows the π…π interactions between imidazole rings and the benzene rings of the two-dimensional layers.

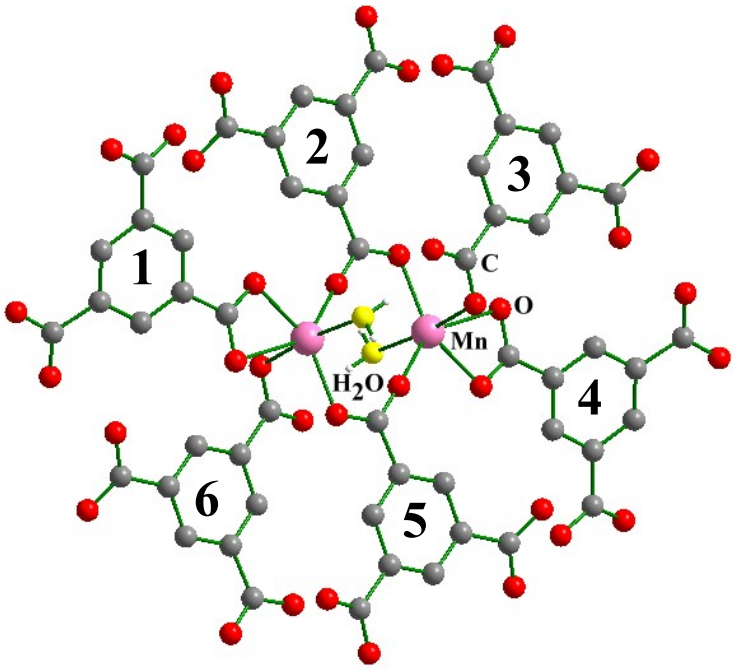


(a)

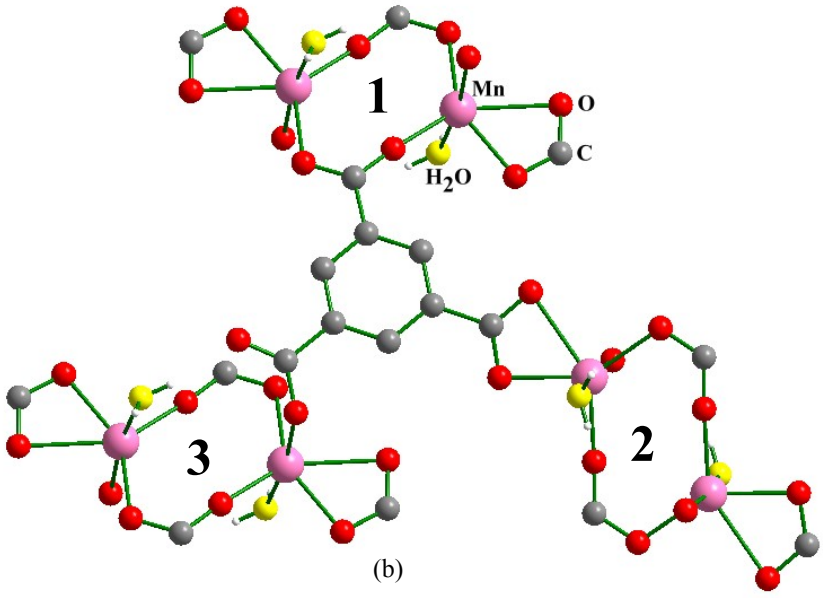


(b)

Fig. S6: (a) Figure shows that each $Mn_2$ dimer is connected six different trimesate anions in **I**; (b) Figure shows that each trimesate anion is connected with three different $Mn_2$ dimers in **I**.

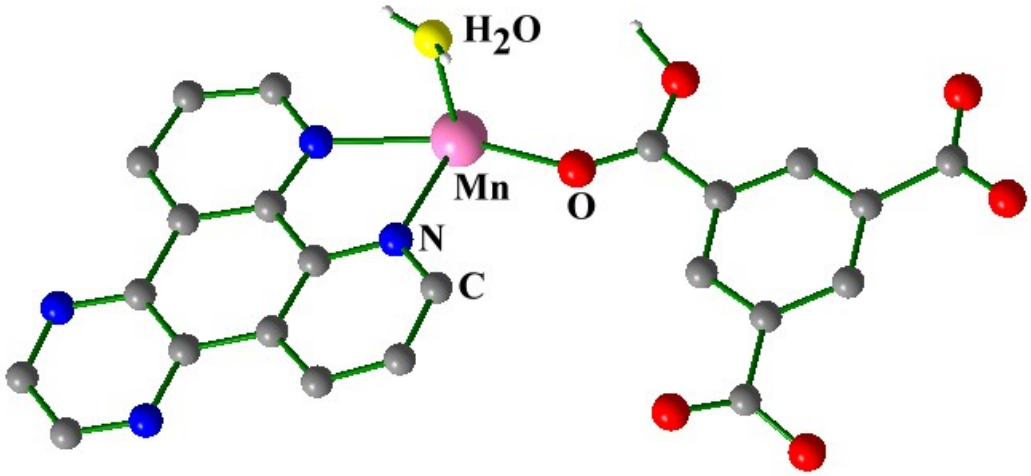


(a)

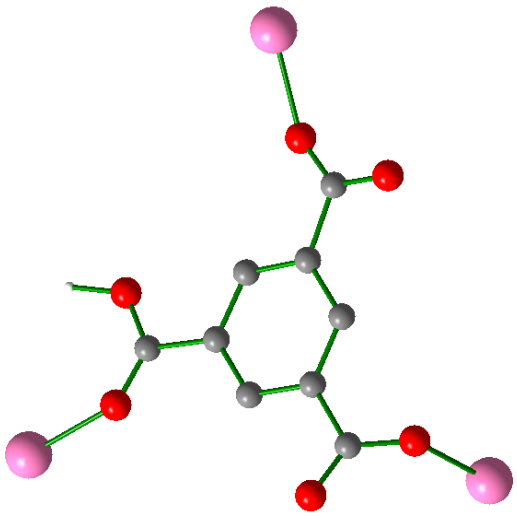

(b)

Fig. S7: (a) The asymmetric unit of [Mn(HBTC)(Pyphen)($H_2O$)] (Pyphen = pyrazino[2,3-f][1,10]-phenanthroline) (Ref. 14); (b) Figure shows the connectivity of HBTC anion with the $Mn^{+2}$ ions in [Mn(HBTC)(Pyphen)($H_2O$)] (Pyphen = pyrazino[2,3-f][1,10]-phenanthroline) (Ref. 14).

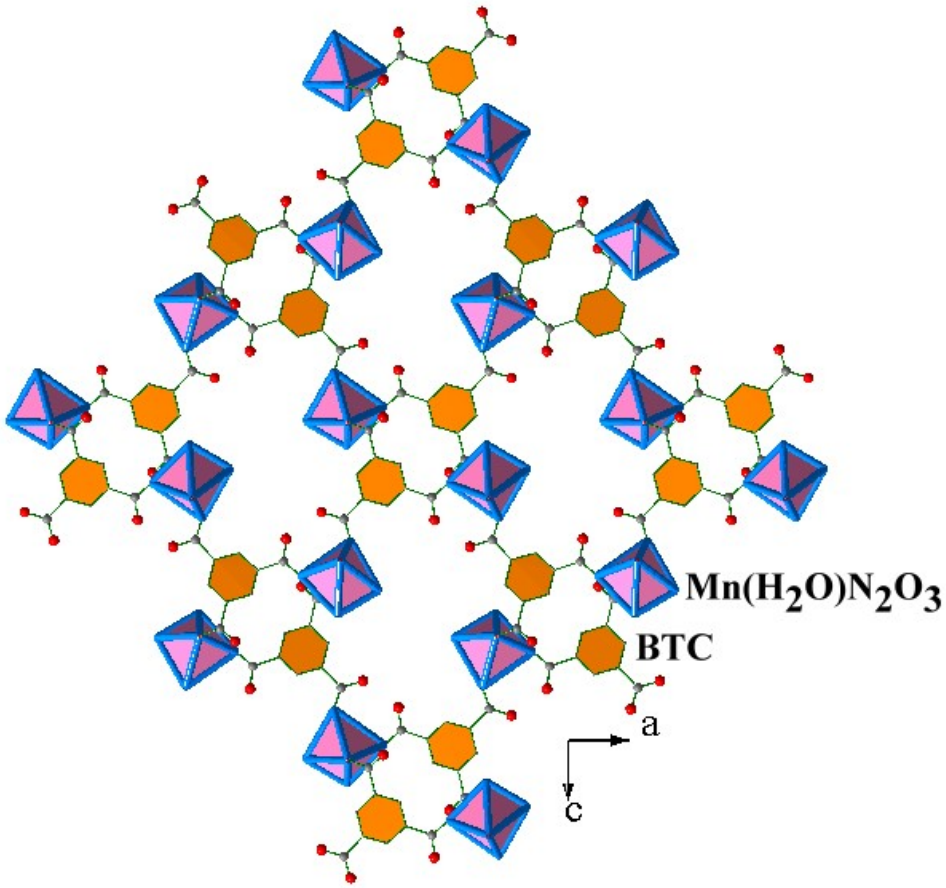


Fig. S8: The polyhedral view of the two-dimensional layer of [Mn(HBTC)(Pyphen)($H_2O$)] (Pyphen = pyrazino[2,3-f][1,10]-phenanthroline) (Ref. 14).

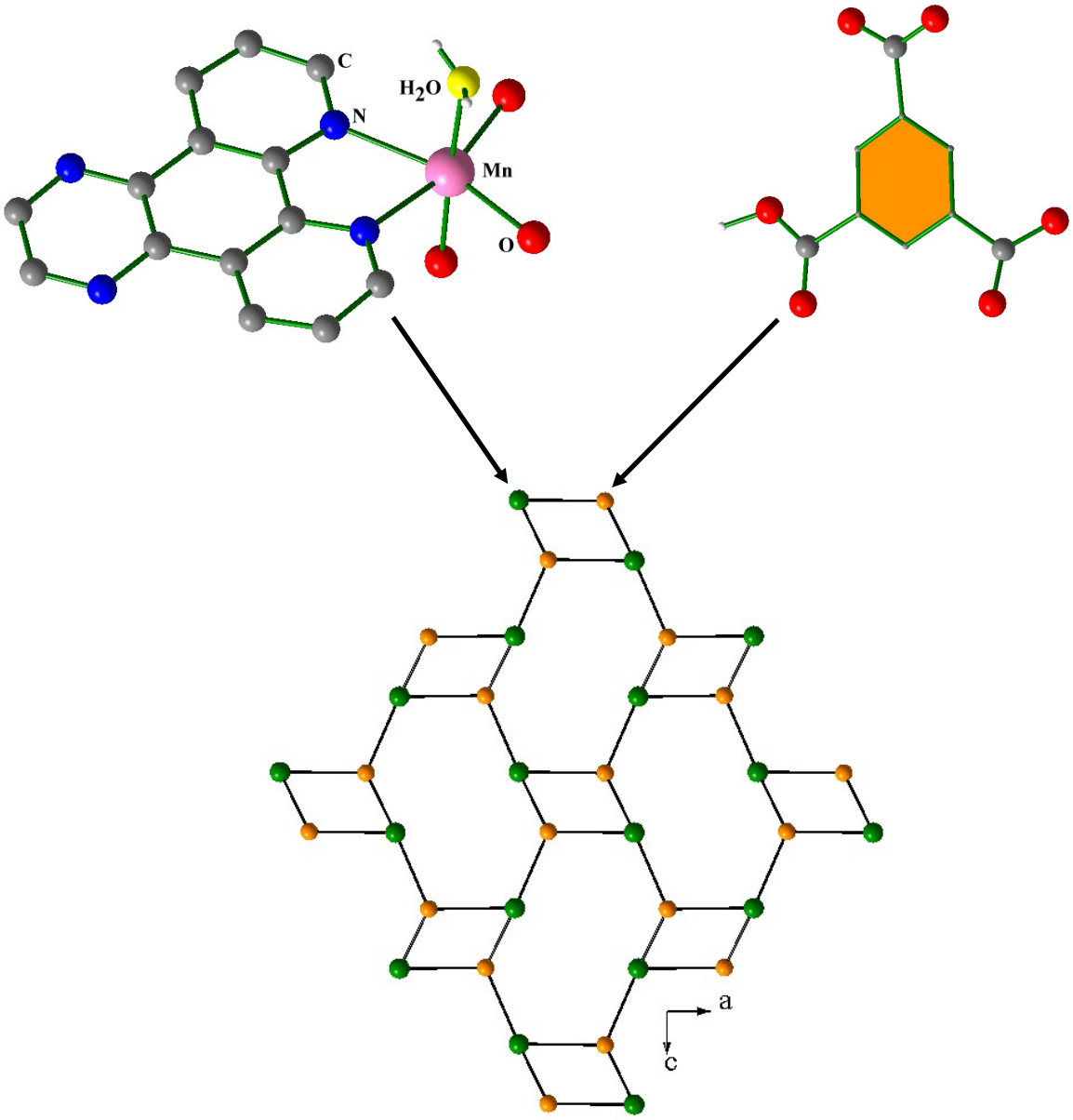


Fig. S9: Schematic representation of the connectivity between the 3-connected $Mn^{+2}$ ions and the 3-connected HBTC anions in[Mn(HBTC)(Pyphen)($H_2O$)] (Pyphen = pyrazino[2,3-f][1,10]-phenanthroline) (Ref. 14).

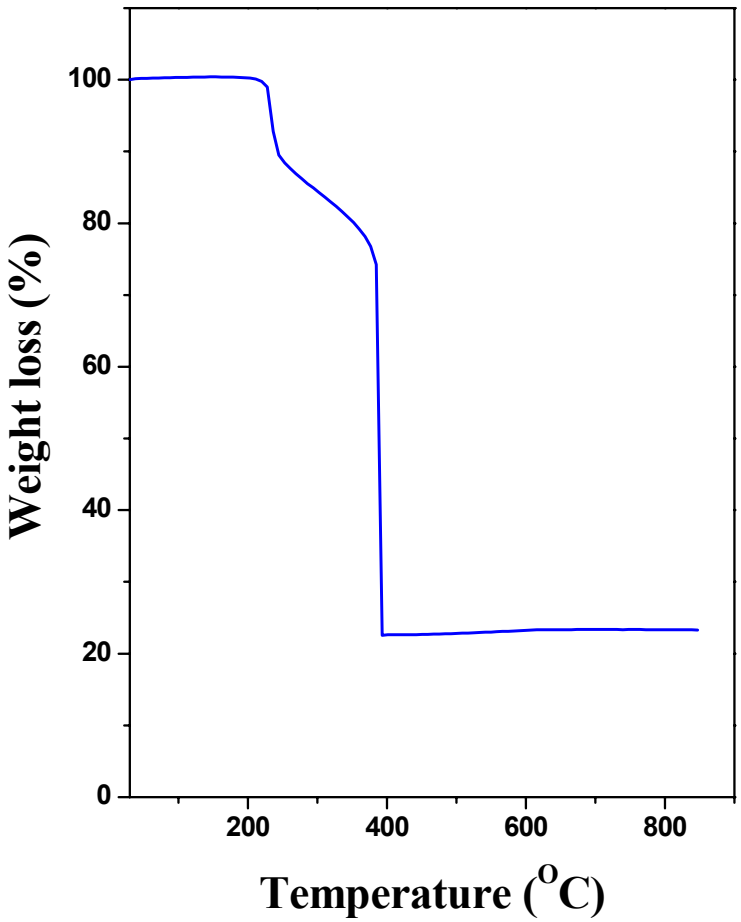


Fig. S10: TGA studies of **I**.

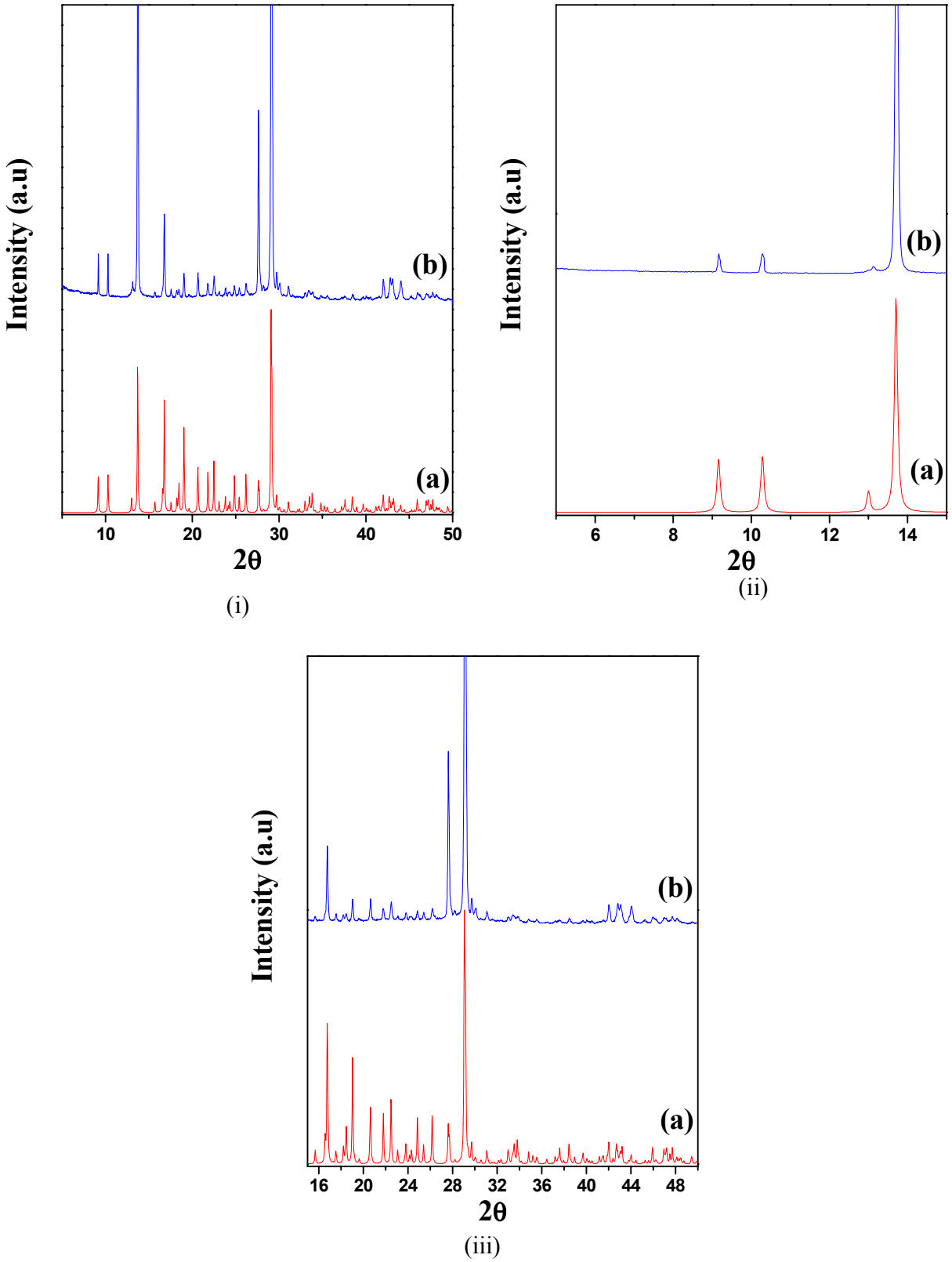


Fig. S11: (i) Powder XRD (CuKα) pattern of **I**, (a) simulated and (b) experimental; (ii) Expanded version of (i) in the range of 5-15°; (iii) Expanded version of (i) in the range 15-50°.

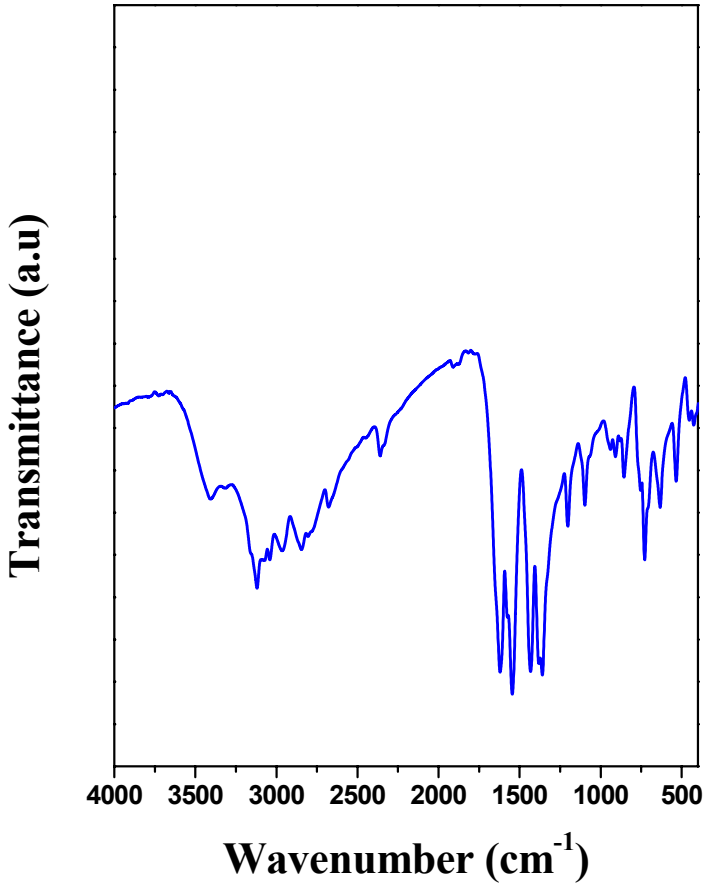


Fig. S12: IR spectra of **I**.

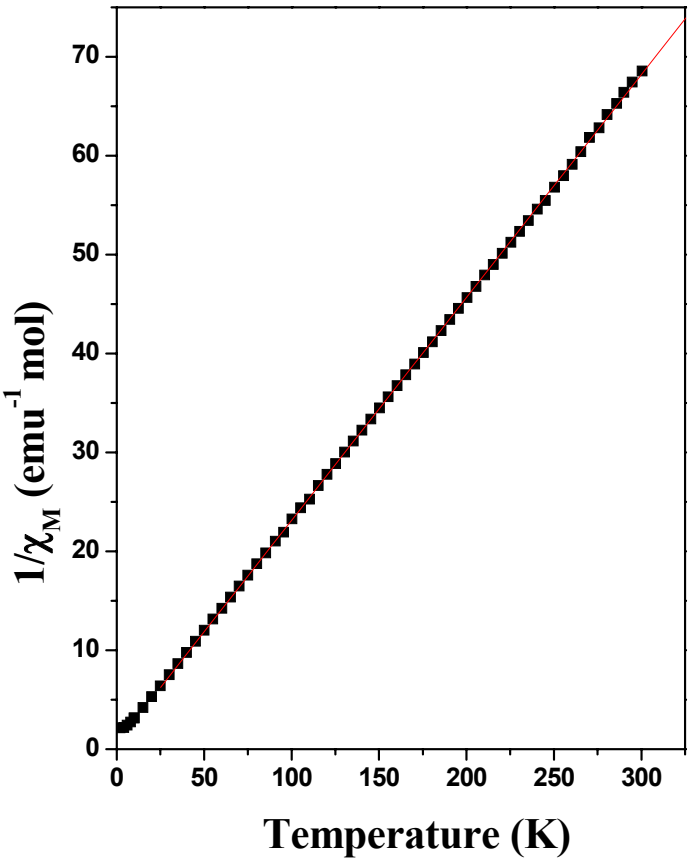


Fig. S13: The temperature variation of the inverse molar susceptibility ($1/\chi_M$) for **I** with Curie-Weiss fit (H = 0.1 T).